Robust multi-objective optimization of safety barriers performance parameters for NaTech scenarios risk assessment and management

Francesco Di Maio[a*], Stefano Marchetti[a], Enrico Zio[a,b]

[a]Energy Department, Politecnico di Milano, Via La Masa 34, Milano 20156, Italy
[b]MINES ParisTech, PSL Research University, CRC, Sophia Antipolis, France

Abstract

Safety barriers are to be designed to bring the largest benefit in terms of accidental scenarios consequences mitigation at the most reasonable cost. In this paper, we formulate the problem of the identification of the optimal performance parameters of the barriers that can at the same time allow for the consequences mitigation of Natural Technological (NaTech) accidental scenarios at reasonable cost as a Multi-Objective Optimization (MOO) problem. The MOO is solved for a case study of literature, consisting in a chemical facility composed by three tanks filled with flammable substances and equipped with six safety barriers (active, passive and procedural), exposed to NaTech scenarios triggered by either severe floods or earthquakes. The performance of the barriers is evaluated by a phenomenological dynamic model that mimics the realistic response of the system. The uncertainty of the relevant parameters of the model (i.e., the response time of active and procedural barriers and the effectiveness of the barriers) is accounted for in the optimization, to provide robust solutions. Results for this case study suggest that the NaTech risk is optimally managed by improving the performances of four-out-of-six barriers (three active and one passive). Practical guidelines are provided to retrofit the safety barriers design.

Keywords: Process safety, NaTech accidents, Safety barriers, Dynamic modeling, Robust Multi-Objective Optimization, NSGA-II, MODEA, MOPSO, MSSA.

Acronyms

ETA	Event Tree Analysis
MOO	Multi-Objective Optimization
NSGA-II	Non-dominated Sorting Genetic Algorithm II
MODEA	Multi-Objective Differential Evolution Algorithm
MOPSO	Multi-Objective Particle Swarm Optimization
MSSA	Multi-objective Salp Swarm Algorithm
HD	Hyperarea Difference
PFD	Probability of Failure on Demand
WDS	Water Deluge System
PFP	Passive Fire Protection
ETI	Emergency Team Intervention
PSV	Pressure Safety Valve
FWS	Foam-Water Sprinkler
MOEA	Multi-Objective Evolutionary Algorithm
IE	Initiating Event
LOC	Loss of Containment
TFM	Time of Final Mitigation
TTF	Time To Failure
FTA	Fault Tree Analysis
RFTA	Reverse Fault Tree Analysis
PDF	Probability Density Function
CR	Crossover Rate
MR	Mutation Rate

Symbols

i	Index of safety barrier
j	Index of natural event
s	Index of escalation scenario
d	Index of decision variable
o	Index of objective function
p	Index of Pareto Front
ϕ	Performance modification factor
f	Objective function
P	Probability of the escalation scenario

Δ_f	Measure of the perturbation of the objective function
HD_p	Hyperarea Difference of the *p-th* Pareto Front
E_p	Set of solutions of the *p-th* Pareto Front
I_p^a	Zone of influence of the *a-th* solution of the *p-th* Pareto Front
$\mu(I_p)$	Measure of the uniformity of the solutions of the *p-th* Pareto Front
$G(E_p)$	G-Metric of the *p-th* Pareto Front
$M_{3,p}^*$	M_3^* Zitzler metric of the *p-th* Pareto Front
$R_{sum,p}$	Aggregation of the rankings of the *p-th* Pareto Front
$t_{r,i}$	Response time of the *i-th* safety barrier
γ_i	Heat radiation reduction factor of the *i-th* safety barrier
σ_y	Yield strength
σ_e	Equivalent stress
Π_s	Performance metric of the *s-th* scenario
Π	Global performance metric
C_T	Cost of the improvement
ω	Parameter for the desired level of robustness of the solutions
δ_d	Min-max normalization of the variation of the *d-th* decision variable

1. Introduction

Accidental scenarios triggered by Natural events and impacting on Technological installations (NaTech scenarios) [1] are a primary concern for industry, due to their probability of escalation to severe consequences and the difficulties of recovery [2]. Safety barriers are installed for preventing technological accidents and mitigating their consequences. To account for their possible performance degradation, due to the impact of natural events, a performance modification factor ϕ is introduced to consider the probability that the barrier is unavailable due to the direct impact of an occurred natural event [3]. The performance modification factor is commonly estimated by expert elicitation [4] and modulates the safety barrier availability, and, eventually, the probability of the accident scenario escalation to severe consequences.

Recent research efforts have introduced specific NaTech risk assessment and management frameworks [5]. However, no methodology has been proposed for identifying the set of improvements to the safety barriers of a given system, whose performance degrades in time, to manage the risk arising from NaTech scenarios. This may also inform retrofitting actions to improve the safety barriers design.

In the present work we propose a novel comprehensive framework for the identification of the safety barriers whose design improvement brings the largest benefit of NaTech scenarios mitigation at the lowest cost. The work is formulated as a Multi-Objective Optimization (MOO) problem to find the optimal values of the safety barriers performance parameters (namely, the Probability of Failure on Demand (PFD) and the performance modification factor). A tailored phenomenological dynamic

model is used to realistically simulate the response of the system when impacted by the NaTech scenario. The MOO searches for the optimal decision variables (the barriers performance parameters) that optimize a set of objective functions (the mitigative power of the system and the cost of the improvements) under constraints (the allowed values of the performance parameters) [6]. To give due account to the uncertainty of some parameters of the dynamic model used for the assessment of the NaTech scenario evolution (i.e., the response times of active and procedural barriers, and the effectiveness of the barriers), an additional constraint is added to the MOO problem, which ensures the achievement of a robust Pareto Front (PF), whose solutions are only marginally affected by the uncertain parameters perturbation [7]. To find the algorithm most suited to solve this problem, four different consolidated MOO algorithms have been benchmarked: Non-dominated Sorting Genetic Algorithm II (NSGA-II) [8], Multi-Objective Differential Evolution Algorithm (MODEA) [9] (which are state-of-practice evolutionary algorithms), Multi-Objective Particle Swarm Optimization (MOPSO) [10] and Multi-objective Salp Swarm Algorithm (MSSA) [11] (which are state-of-practice swarm intelligence algorithms). Each one releases a set of Pareto-optimal solutions, that compose the PFs [12], which are compared with respect to three metrics of literature [13], namely the Hyperarea Difference (HD) [14], which corresponds to the area dominated by the PF, the G-metric [15], which accounts both for the level of domination of the PF points and for their distribution in the solution space, and the M_3^* Zitzler metric (M_3^*) [16], which accounts for the extension of the PF in the solution space. Eventually, the most suited algorithm to solve the problem is used to obtain the robust PF, which is used to find the safety barriers that are pivotal to get the maximum mitigative power with the lowest cost: by so doing, the analyst is provided with all the information needed to retrofit the design to these outcomes and, therefore, properly manage the NaTech risk.

An application of the proposed framework is shown with respect to a case study of literature [3] that consists of a chemical facility composed by three tanks and equipped with $i = 1,2,3,4,5$ different safety barriers (active, passive and procedural), respectively: Water Deluge System (WDS), Passive Fire Protection material (PFP), Emergency Team Intervention (ETI), Foam-Water Sprinkler system (FWS) and Pressure Safety Valve (PSV). In [4], a group of 38 experts are asked to assess the impact of floods and earthquakes ($j = 1,2$, respectively) on the availability of the $i = 1,2,3,4,5$ safety barriers, in order to estimate their performance modification factor $\phi_{j,i}$ and calculate its effect on the Probability of Failure on Demand ($PFD_{0,i}$), that is the probability that the barrier is found unavailable upon demand. This latter is here finally used to estimate the probability $P_{j,s}$ of the $s = 1,2,\dots,S$ escalation scenarios triggered by the *j-th* natural event. For this, we develop an Event Tree Analysis (ETA) that drives the simulations of a dynamic model of literature [17] for determining the structural integrity of the tanks when impacted by the NaTech scenario. The safety barriers parameters to be improved for reaching the safety goals are identified by the proposed MOO-based framework and practical guidelines are provided to retrofit the safety barriers design for optimally managing the risk arising from the considered NaTech scenarios.

The remainder of the paper is organized as follows: Section 2 illustrates the proposed framework; Section 3 presents the case study; Section 4 shows the results of the application of the proposed method to the case study; in Section 5, conclusions are drawn.

2. The Multi-Objective Optimization framework

We consider a set of N safety barriers, whose contribution to the mitigation of the accidental scenario escalation is typically assessed with a site-specific phenomenological dynamic model, in which each barrier is characterized by $PFD_{0,i}$, which is modified by $\phi_{j,i}$ ($j = 1, 2, \dots, J$ and $i = 1, 2, \dots, N$), that is the probability that the *i-th* safety barrier is not available due to the direct impact of the *j-th* natural hazard [4] as follows:

- Active barriers:

$$PFD_{j,i} = 1 + (\phi_{j,i} - 1)(1 - PFD_{0,i}) \tag{1}$$

- Passive barriers:

$$PFD_{j,i} = \phi_{j,i} \tag{2}$$

   since, for passive barriers, $PFD_{0,i} = 0$ [3].

- Procedural barriers: the definition must be tailored on the specific safety procedure; as an example, the performance of ETI (hereafter considered in the case study) should consider both $PFD_{j,ETI}$ and the Time of Final Mitigation (TFM) of the NaTech scenario:

   i. $PFD_{j,ETI} = 1 + (\phi_{j,ETI} - 1)(1 - PFD_{0,i})$ (similarly to an active barrier).

   ii. $TFM \gg TFM_0$, to take into account the hindrance coming from the unfavorable environmental conditions [3], where TFM_0 is the value typically considered for conventional scenarios.

The proposed optimization framework is comprised of the following steps:

1. Define a MOO problem to search for the optimal values of $\phi_{j,i}$ and $PFD_{0,i}$ in terms of cost and mitigative power of the system, while also accounting for the uncertainties in the estimation of the mitigative power;

2. Identify the MOO algorithm most suited for the problem by comparing four state-of-practice algorithms (namely, NSGA-II, MODEA, MOPSO and MSSA) with respect to three metrics (namely, HD, G-metric and M_3^*);

3. Analyze the robust PF (released by the most suited algorithm) to identify the safety barriers that are pivotal to get the maximum mitigative power with the minimum cost and provide practical guidelines to retrofit the safety barriers design to the requirements in the parameters.

2.1. *MOO problem definition*

The first step of the framework requires the definition of the MOO problem, which is composed of:

- A set of decision variables $d = 1, 2, \dots, D$ (i.e., $PFD_{0,i}$ and $\phi_{j,i}$ of each barrier).

- A set of objective functions (f_o, with $o = 1,2$): a measure of the mitigative power of the system, evaluated with a tailored site-specific phenomenological dynamic model, and the total

cost of the improvements, determined with a dedicated analysis to identify the set of actions necessary to improve $PFD_{0,i}$ and $\phi_{j,i}$.

- A set of constraints $c = 1,2,\dots,C$, that are problem-specific, and consist in:

  - The allowed values of the safety barriers performance parameters;

  - A maximum allowed perturbation of the *o-th* objective:

  $$\Delta_{f_o} \leq \omega \tag{3}$$

  where the parameter ω can be set to achieve the desired level of robustness of the solutions and Δ_{f_o} is a measure of the perturbation of the *o-th* objective, defined as in [7]:

  $$\Delta_{f_o} = \frac{|f_o^p - f_o|}{f_o} \tag{4}$$

  where f_o^p is the worst (i.e., highest) value of f_o that can be obtained perturbing the uncertain parameters within their uncertainty range. This allows finding only the robust solutions, here defined as those marginally affected by the perturbation of the uncertain parameters.

2.2 Identification of the most suited algorithm

Different MOO algorithms can be used (those considered in the present work are described in the Appendix, being state-of-practice algorithms that do not add novelty to the framework) and benchmarked on the MOO problem defined in Section 2.1, neglecting the robustness (Eq. (3)) for the sake of computational time saving. The set of $p = 1,2,3,4$ PFs released by the selected MOO algorithms are compared with respect to:

1. HD, which is defined as the area dominated by each PF, and calculated as follows [18]:

$$HD_p = \sum_{a=1}^{NS_p} \left(1 - \overline{f_{1,p}^a}\right)\left(\overline{f_{2,p}^{a+1}} - \overline{f_{2,p}^a}\right) + \left(1 - \overline{f_{1,p}^a}\right)\left(1 - \overline{f_{2,p}^a}\right) \tag{5}$$

where $\overline{f_{1,p}^a}$ and $\overline{f_{2,p}^a}$ are the values (after a min-max normalization) of the objective functions for the *a-th* solution of the *p-th* PF, respectively, and NS_p is the total number of solutions in the *p-th* PF. Then, the ranking H_p is obtained by sorting them with respect to HD_p in descending order.

2. G-Metric, which accounts both for the level of domination of the points of one PF with respect to the others and for their distribution in the objective space, and is calculated as follows [15]:

a. Normalize all the PFs with a min-max normalization using the maximum and minimum values of the two objective functions of the union $C = \bigcup_{p=1}^{4} E_p$, where E_p represents the set of solutions of the *p-th* PF.

b. Divide the PFs in K levels L_k that represent levels of complete domination (i.e., all the solutions of the PFs in level L_{k+1} are dominated by at least one solution of the PFs in level L_k).

c. For each level L_k and for each $E_p \in L_k$:

    i. Eliminate all solutions $a \in E_p$ dominated by any other solution belonging to a PF of the same level.

    ii. For each solution $a \in E_p$, find the set of solutions (Q_a) that belong to its zone of influence I_p^a, which correspond to the solutions u with $d(u, a) \leq U$, where $d(u, a)$ is the distance from a and the radius U is empirically determined.

    iii. Calculate the measure of the uniformity of the distribution of the solutions $(\mu(I_{E_p}))$ as follows:

$$\mu(I_{E_P}) = \sum_{a=1}^{NS_p} 2 \int_{Q_a} \sqrt{U^2 - d(u,a)^2} \, dQ_a \tag{6}$$

d. For each $E_p \in L_k$, calculate the value of the G-Metric as follows:

$$G(E_p) = \mu(I_{E_p}) + \sum_{k^*=k+1}^{K} \mu_{max}(L_{k^*}) \tag{7}$$

where $\mu_{max}(L_{k^*})$ is the maximum value of $\mu(I_{E_P})$ for all $E_p \in L_{k^*}$. Finally, the ranking G_p is obtained by sorting them with respect to $G(E_p)$ in descending order.

3. M_3^*, which accounts for the extension of the PF in the objective space and is calculated as follows [16]:

$$M_{3,p}^* = \sqrt{(max\{\overline{f_{1,p}}\} - min\{\overline{f_{1,p}}\}) + (max\{\overline{f_{2,p}}\} - min\{\overline{f_{2,p}}\})} \tag{8}$$

Then, the ranking M_p is obtained by sorting them with respect to $M_{3,p}^*$ in descending order.

To find the most suited algorithm, the individual rankings produced by the three metrics are summed in $R_{sum,p}$, without any preference weight:

$$R_{sum,p} = H_p + G_p + M_p \tag{9}$$

and, then, sorted in descending order to find the algorithm most suited to the problem.

The identified algorithm is then used to solve the MOO problem of Section 2.1 with the inclusion of the robustness constraint of Eq. (3), releasing a robust PF whose solutions are each constituted by a set of optimal values of $PFD_{0,i}$ and $\phi_{j,i}$.

2.3 *Pareto front analysis and practical design guidelines*

To find which performance parameters have to be improved, the Probability Density Function (PDF) of the difference between the initial values of $PFD_{0,i}$ and $\phi_{j,i}$ and those of the solutions of the robust PF are calculated and analyzed. Then, the following guidelines can be complied to inform the retrofitting of the safety barriers design by targeting the expectations of the results of the robust PF:

- To reach the value of $PFD_{0,i}$ equal to one of those leading to the robust PF solutions, a Reverse Fault Tree Analysis (RFTA) [19] can be used, by setting the top event probability equal to the desired value of $PFD_{0,i}$ and finding the probabilities of the basic events that allow obtaining it ([20], [21]);

- To reach the value of $\phi_{j,i}$ equal to one of those leading to the robust PF solutions, a site-specific analysis is needed, since it is strongly affected by the specific environmental conditions of the site and by the type and safety function of the barrier. As an example, we can mention the analysis performed to target WDS: since the unavailability of this barrier during NaTech scenarios is mostly due to the loss of external power [22], the installation of a backup power unit on site, if not already present, would lead to an improvement of $\phi_{j,WDS}$.

3. Case study

3.1. *Overview*

The layout of the considered chemical facility of literature [3] is shown in **Fig. 1**. It is composed of two atmospheric tanks (T1 and T2) that store liquid flammable substances and one pressurized vessel (P1) that contains liquid petroleum gas. The chemical facility is exposed to severe floods and earthquakes, here assumed, without loss of generality, both with a return period of 500 years, and characterized by a prototypical flood water depth of The chemical facility is exposed to severe floods and earthquakes, here assumed, without loss of generality, both with a return period of 500 years, and characterized by a prototypical flood water depth of 2 m and a peak ground acceleration of $4.9 \frac{m}{s^2}$, respectively. For the sake of brevity, the proposed framework is applied (and the results shown) only with respect to NaTech scenarios triggered by earthquakes; therefore, in what follows, the index j is dropped throughout the analysis.
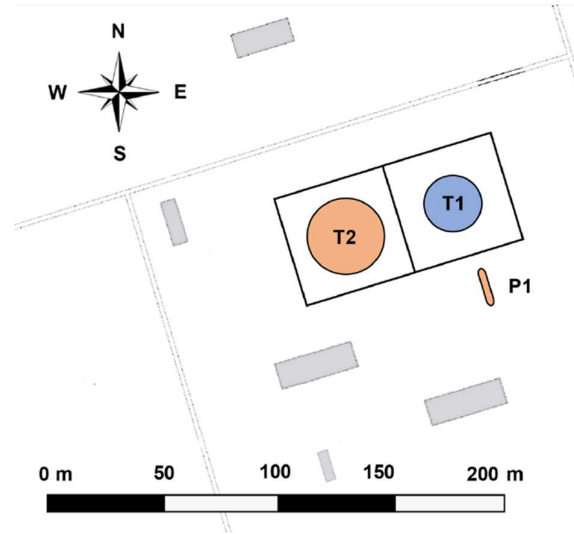
Fig. 1. Layout of the considered case study [3].

The considered Initiating Event (IE) of the NaTech scenario consists in a Loss of Containment (LOC) of T1 that leads to a pool fire affecting P1 and T2, and occurs at time $t = 0\ s$. The safety barriers designed and implemented in P1 and T2 to withstand the escalation of the accidental scenario are listed in **Tab. 1**. Among these, WDS, FWS and PSV are active, PFP is passive, and ETI is a procedural barrier. ETI is considered to be in common between the two tanks, meaning that it will only be optimized once by the MOO algorithm.

Safety Barrier	Classification	P1	T2	Description
1) Water deluge system (WDS)	Active	X		Water delivery during fire
2) Passive fire protection material (PFP)	Passive	X		Coating fireproof material
3) Pressure safety valve (PSV)	Active	X	X	Valve designed to relieve excess pressure
4) Emergency team intervention (ETI)	Procedural	X	X	Emergency firefighter team intervention
5) Foam-Water Sprinkler system (FWS)	Active		X	Foam delivery during fire

Tab. 1. Safety barriers considered in the case study.

The values of ϕ_i of these safety barriers in case of earthquake, which result from a survey involving 38 experts, are taken from [4] and are used to modify the performance of the barriers as described in Section 2.

The ETs shown in **Fig. 2** and **Fig. 3** delineate the different scenarios initiated by the IE, spooned by the success or failure of the safety barriers and involving P1 and T2, respectively. Each scenario involving P1 is, then, combined with each scenario involving T2, as in the example of **Fig. 4**, to obtain the $S = 128$ scenarios involving both tanks and to calculate their probability P_s.
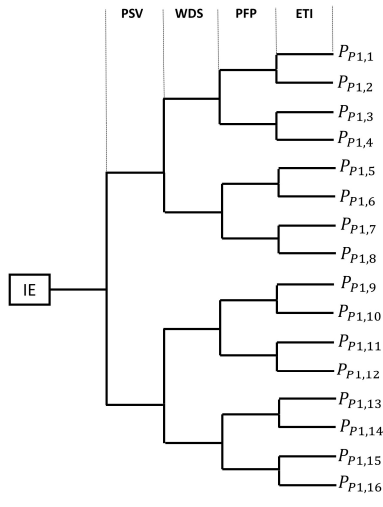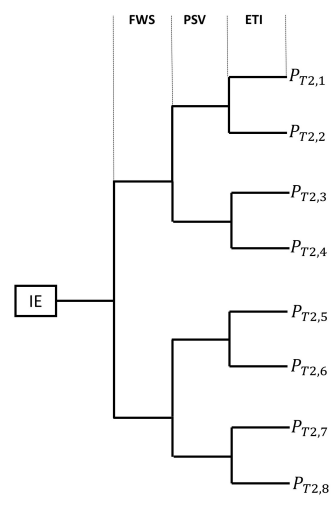
Fig. 2. ET that delineates the scenarios involving P1.
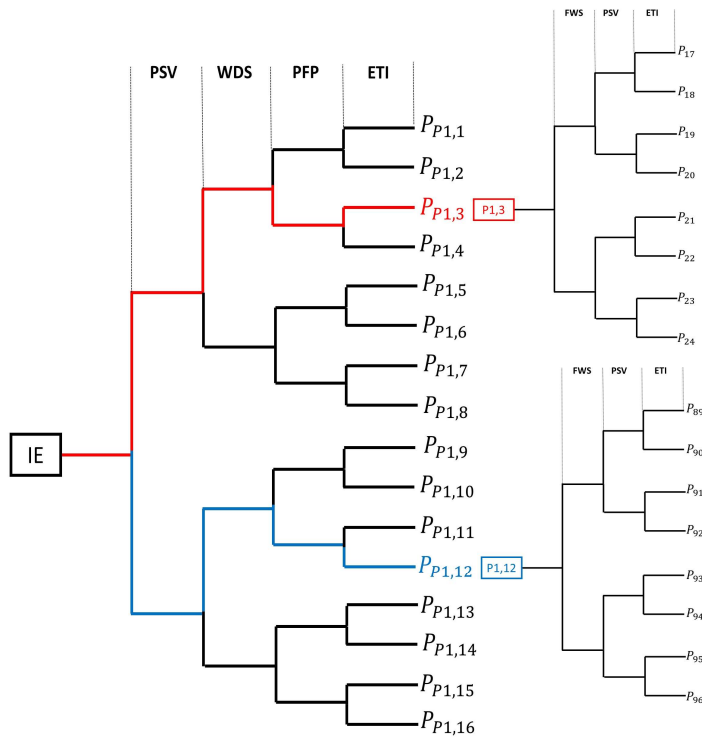

Fig. 3. ET that delineates the scenarios involving T2.

FWS PSV ETI

PSV WDS PFP ETI

$P_{P1,1}$
$P_{P1,2}$
$P_{P1,3}$ P1,3
$P_{P1,4}$
$P_{P1,5}$
$P_{P1,6}$
$P_{P1,7}$
$P_{P1,8}$
$P_{P1,9}$
$P_{P1,10}$
$P_{P1,11}$
$P_{P1,12}$ P1,12
$P_{P1,13}$
$P_{P1,14}$
$P_{P1,15}$
$P_{P1,16}$

IE

P_{17}
P_{18}
P_{19}
P_{20}
P_{21}
P_{22}
P_{23}
P_{24}

FWS PSV ETI

P_{89}
P_{90}
P_{91}
P_{92}
P_{93}
P_{94}
P_{95}
P_{96}

Fig. 4. Example of combination of the scenarios involving P1 and T2.

3.2. The phenomenological dynamic model

A phenomenological dynamic model of literature [17] has been tailored to the case study to evaluate the NaTech scenario evolution after the IE and determine the system mitigative power. This model, whose steps are reported in the flowchart of **Fig. 3**, allows estimating the structural integrity of the two tanks (whose physical properties are reported in **Tab. 2**) when hit by the fire triggered by the IE.

Tank	Volume	Thickness	Diameter	Specific Heat	Density	Storage Mass	Op. pressure	Yield strength
P1	$105\ m^3$	$0.007\ m$	$2.6\ m$	$0.5\ \dfrac{kJ}{kg \cdot K}$	$7900\ \dfrac{kg}{m^3}$	$52\ ton$	$8.34\ bar$	$235\ MPa$
T2	$4300\ m^3$	$0.01\ m$	$32\ m$	$0.5\ \dfrac{kJ}{kg \cdot K}$	$7900\ \dfrac{kg}{m^3}$	$3000\ ton$	$1\ bar$	$235\ MPa$

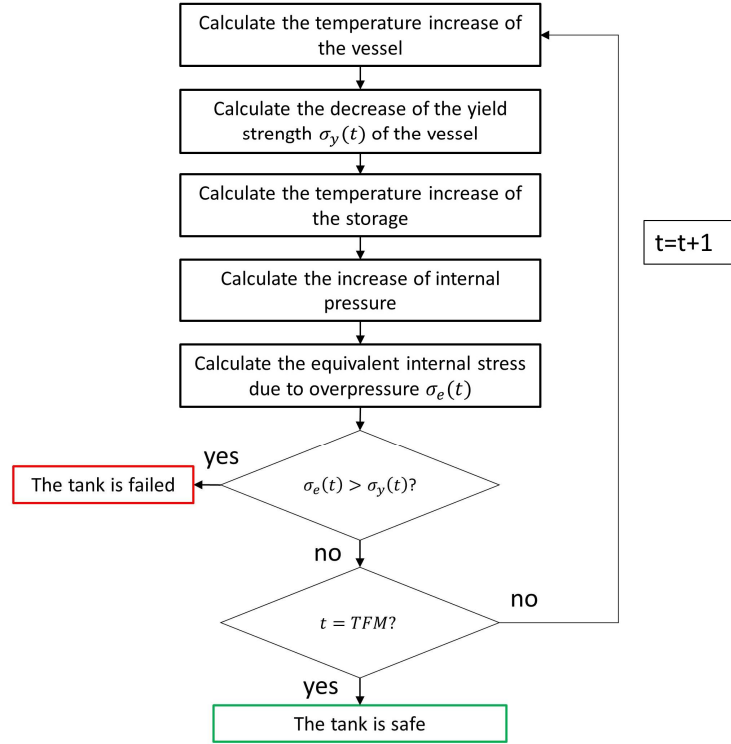**Tab. 2**. Physical properties of the tanks.

Fig. 3. Flowchart of the dynamic model.

Each one of the safety barriers implemented in the system contributes to the mitigation of the accidental scenario after its response time $t_{r,i}$, as described in **Tab. 3**.

Safety Barrier	Mitigative Action	Response Time	Uncertainty Range
1) WDS	Reduction of the heat radiation by a factor $\gamma_{WDS} = 0.5$ [20].	$t_{r,WDS} = 220\ s$ ([23], [24])	$t_{r,WDS} \in [182, 272]$ s ([23], [24]) $\gamma_{WDS} \in [0.35, 0.85]$ [20]
2) PFP	Reduction of the vessel temperature increase (thermal properties from [25]).	$t_{r,PFP} = 0\ s$	-
3) PSV	Increase of the system tolerance to overpressure.	$t_{r,PSV} = 6.5\ ms$ [26]	$t_{r,PSV} \in [5.9, 7.8]$ ms [26]
4) ETI	Reduction of the heat radiation by a factor $\gamma_{ETI} = 0.6$ [20].	$t_{r,ETI} = 780\ s$ [27]	$t_{r,ETI} \in [420, 1020]$ s [27] $\gamma_{ETI} \in [0.45, 0.95]$ [20]
5) FWS	Reduction of the heat radiation by a factor $\gamma_{WDS} = 0.5$ [20].	$t_{r,FWS} = 220\ s$ ([23], [24])	$t_{r,FWS} \in [182, 272]$ s ([23], [24]) $\gamma_{FWS} \in [0.35, 0.85]$ [20]

Tab. 3. Safety barriers mitigative action and uncertainty range of the parameters.

The mitigative power of the safety barriers is firstly mapped into a performance metric that represents, for each *s-th* scenario, the minimum structural integrity among the tanks:

$$\Pi_s(t) = \min_b \left(\frac{\sigma_{y,b,s}(t) - \sigma_{e,b,s}(t)}{\sigma_{y,b,s}(t)} \right) \tag{11}$$

where $\sigma_{y,b,s}(t)$ and $\sigma_{e,b,s}(t)$ are, respectively, the yield strength and the equivalent stress at time t of the *b-th* tank in the *s-th* scenario, and then, into a "global" performance metric, which weights the Π_s of failure scenarios (i.e., scenarios in which at least one of the tanks fail) with their probability of occurrence P_s :

$$\Pi = \sum_{f=1}^{N_f} \left(\int_{t=0}^{t=TFM} \Pi_s(t)\, dt \right) \cdot P_s \tag{12}$$

where N_f is the number of failure scenarios and $TFM = 400\ min$ [3].

Since the mitigative power has to be maximized, the f_1 to be minimized is written as follows:

$$f_1 = \frac{1}{\Pi} \tag{13}$$

In other words, we can say that the MOO will search for those safety barriers performance parameters capable of reducing the occurrence of the failure scenarios most harming the tanks structural integrity (i.e., the worst-case scenarios).

3.3. Cost of the improvements of the safety barriers

The costs of the improvement of $PFD_{0,i}$ and ϕ_i ($C_{PFD,i}$ and C_{ϕ_i}, respectively), are considered asymptotically larger starting from a minimum of $PFD_{0,i,in}$ and $\phi_{i,in}$, that $PFD_{0,i}$ and ϕ_i take as their initial value as in [28]:

$$C_{PFD,i}(PFD_{0,i}) = \frac{A_i}{PFD_{0,i}} \tag{14}$$

$$C_{\phi,i}(\phi_i) = \frac{B_i}{\phi_i} \tag{15}$$

The total cost for the improvements is calculated as in Eq. (16):

$$C_T = \int_{PFD_{0,i}}^{PFD_{0,i,in}} C_{PFD,i}(PFD_{0,i})\, d\, PFD_{0,i} + \int_{\phi_i}^{\phi_{i,in}} C_{\phi,i}(\phi_i)\, d\phi_i \tag{16}$$

where A_i and B_i are constants that are estimated, as listed in **Tab. 4**, assuming that:

- Active barriers:
    - The cost for the improvement of $PFD_{0,i}$ of active barriers is of the same order of magnitude of the initial cost of the safety barrier, leading to $A_{WDS} = 3 \cdot 10^4$, $A_{FWS} = 10^5$ € [29] and $A_{PSV} = 5 \cdot 10^3$ € [30];

- The cost of the improvement of ϕ_{WDS} and ϕ_{FWS} amounts to the cost of the installation of an auxiliary energy source on site, since they rely on external energy sources that are often unavailable during NaTech scenarios [22], leading to $B_{WDS} = B_{FWS} = 5 \cdot 10^4$ €. The improvement of ϕ_{PSV} is assumed to be effective upon the installation of an additional pressure relief device, leading to $B_{PSV} = 5 \cdot 10^3$ € [30].

- Passive barriers: the impact of the earthquake on PFP can cause cracking of the fireproof layer [31], which degrades its performance and can lead to complete failure. Therefore, ϕ_{PFP} can be improved with an increase of its thickness, leading to $B_{PFP} = 6 \cdot 10^4$ € [32].

- Procedural barriers:
    - The improvement of $PFD_{0,ETI}$ can be achieved with the installation of additional fire detection and warning equipment, leading to $A_{ETI} = 10^4$ €;
    - Since the earthquake can lead to the disruption of the water supply [33], ϕ_{ETI} can be improved with the installation of an underground water tank, leading to $B_{ETI} = 10^4$ €.

Safety Barrier	$PFD_{0,i,in}$	$\phi_{i,in}$	A_i	B_i
1) WDS	0.0433	0.75	$3 \cdot 10^4$ €	$5 \cdot 10^4$ €
2) PFP	-	0.25	-	$6 \cdot 10^4$ €
3) PSV	0.01	0	$5 \cdot 10^3$ €	$5 \cdot 10^3$ €
4) ETI	0.1	0.85	10^4 €	10^4 €
5) FWS	0.0053	0.5	10^5 €	$5 \cdot 10^4$ €

Tab. 4. Values of $PFD_{0,i,in}$, $\phi_{i,in}$, A_i and B_i.

Finally, f_2 to be minimized is defined in Eq. (17):

$$f_2 = C_T \tag{17}$$

4. Results

The framework described in Section 2 has been applied to the case study presented in Section 3.
Step 1: the MOO problem has been defined as described in Section 2.1. The decision variables are the values of $PFD_{0,i}$ and ϕ_i of the safety barriers, leading to a total of $D = 11$ decision variables. The objective functions are defined and calculated as presented in Section 3.2 and Section 3.3, the robustness constraint of Eq. (3) is set to $\omega = 0.15$ (that is a problem-specific value here empirically set, without loss of generality) and the adopted constraints for $PFD_{0,i}$ and $\phi_{j,i}$ are reported in **Tab. 5**.

Safety Barrier	Constraints
1) WDS	$PFD_{0,WDS} \leq 4.33 \cdot 10^{-2}$, $\phi_{WDS} \leq 0.75$
2) PFP	$PFD_{0,PFP} = 0$, $\phi_{PFP} \leq 0.25$
3) PSV	$PFD_{0,PSV} \leq 0.01$, $\phi_{PSV} = 0$
4) ETI	$PFD_{0,ETI} \leq 0.1$, $\phi_{ETI} \leq 0.85$
5) FWS	$PFD_{0,FWS} \leq 5.3 \cdot 10^{-3}$, $\phi_{FWS} \leq 0.5$

Tab. 5. Constraints of the MOO problem.

Step 2: the simplified MOO problem is solved employing four algorithms, with the following settings (see Appendix for further details):

1) NSGA-II: $NP_N = 110$, $CR_N = 0.1$, MR $= 0.15$ [34].

2) MODEA: $NP_M = 110$, $CR_M = 0.1$, F $= 0.5$ [9].

3) MOPSO: $NP_P = 53$, $NR_P = 200$, w $= -0.35$ [35].

4) MSSA: $NP_S = 50$, $NR_S = 200$ [11].

The PFs released by the four algorithms are shown in **Fig. 4**.
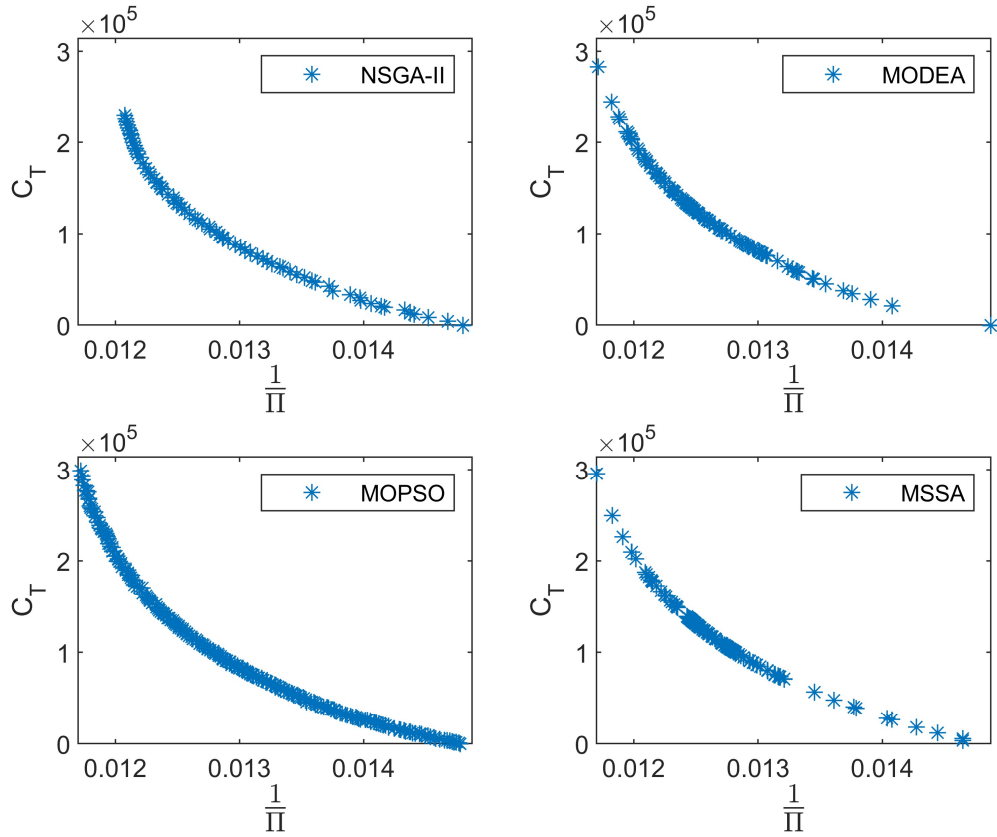
Fig. 4. PFs released by NSGA-II (top-left), MODEA (top-right), MOPSO (bottom-left) and MSSA (bottom-right).

MODEA is identified as the algorithm most suited for the case study, since it is ranked first by all of the three metrics of Section 2.2 (**Fig. 5** and **Tab. 6**), with the following values: $HD_{MODEA} = 0.2529$, $G(A_{MODEA}) = 0.7406$, $M^*_{3,MODEA} = 0.2647$, which are larger than those of all the other algorithms.
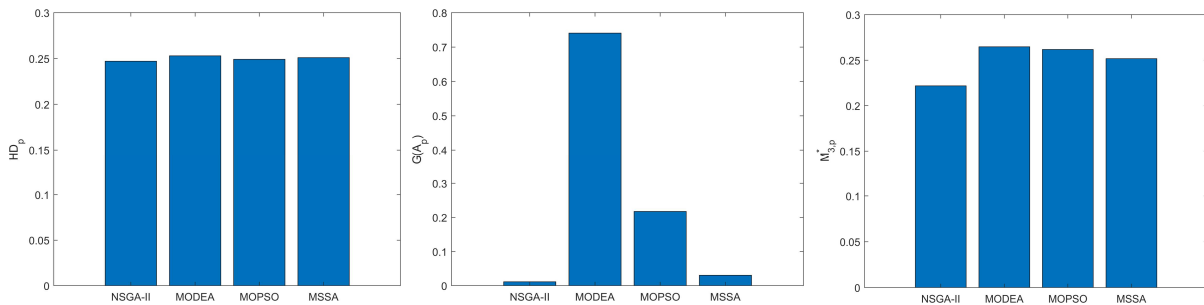

Fig. 5. Results of HD (left), G-Metric (center) and M^*_3 (right).

Metric	MOGA	MODEA	MOPSO	MSSA
HD	0.2470	0.2529	0.2491	0.2509
$G(A)$	0.0114	0.7406	0.2174	0.0305
M_3^*	0.2218	0.2647	0.2618	0.2517

Tab. 6. Numerical results of HD, G-Metric and M_3^*.

In **Fig. 6**, the robust PF provided by MODEA is compared with the PF shown in **Fig. 4** (top right).
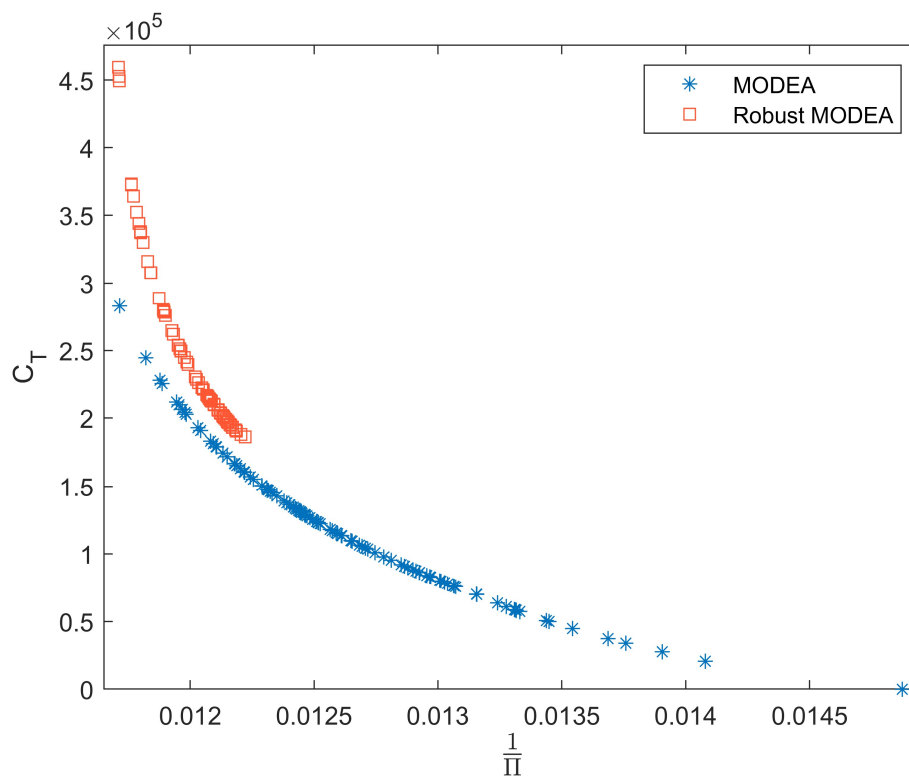

Fig. 6. Comparison between the robust (orange squares) and non-robust (blue stars) PFs released by MODEA.

It can be seen that when the uncertainty of some relevant parameters of the dynamic model is duly propagated throughout the analysis, a minimum cost (equal to $1.86 \cdot 10^5 €$) bounds the domain of the possible optimal solutions (orange squares), and that, incidentally, it is larger than the solution with the same performance of the non-robust PF (blue stars), whose cost is equal to $1.65 \cdot 10^5 €$: this means that neglecting the uncertainties in the phenomenological model would lead to an underestimation of the cost to optimally manage the risk arising from NaTech scenarios or, conversely, an optimistic estimation of the performance when the underestimated budget is allocated, exposing the facility to severe consequences of the NaTech scenario.

Step 3: In **Fig. 7**, the histograms of the PDF of δ_d (i.e., the min-max normalization of the variation of the d-th decision variable from its initial value) of ϕ_{PFP}, ϕ_{ETI}, ϕ_{FWS}, $PFD_{0,PSV,T1}$ and $PFD_{0,PSV,T2}$ (i.e., the parameters that are to be improved the most) are built from both the robust and non-robust PF of MODEA (**Fig. 4** and **Fig. 6**, respectively).
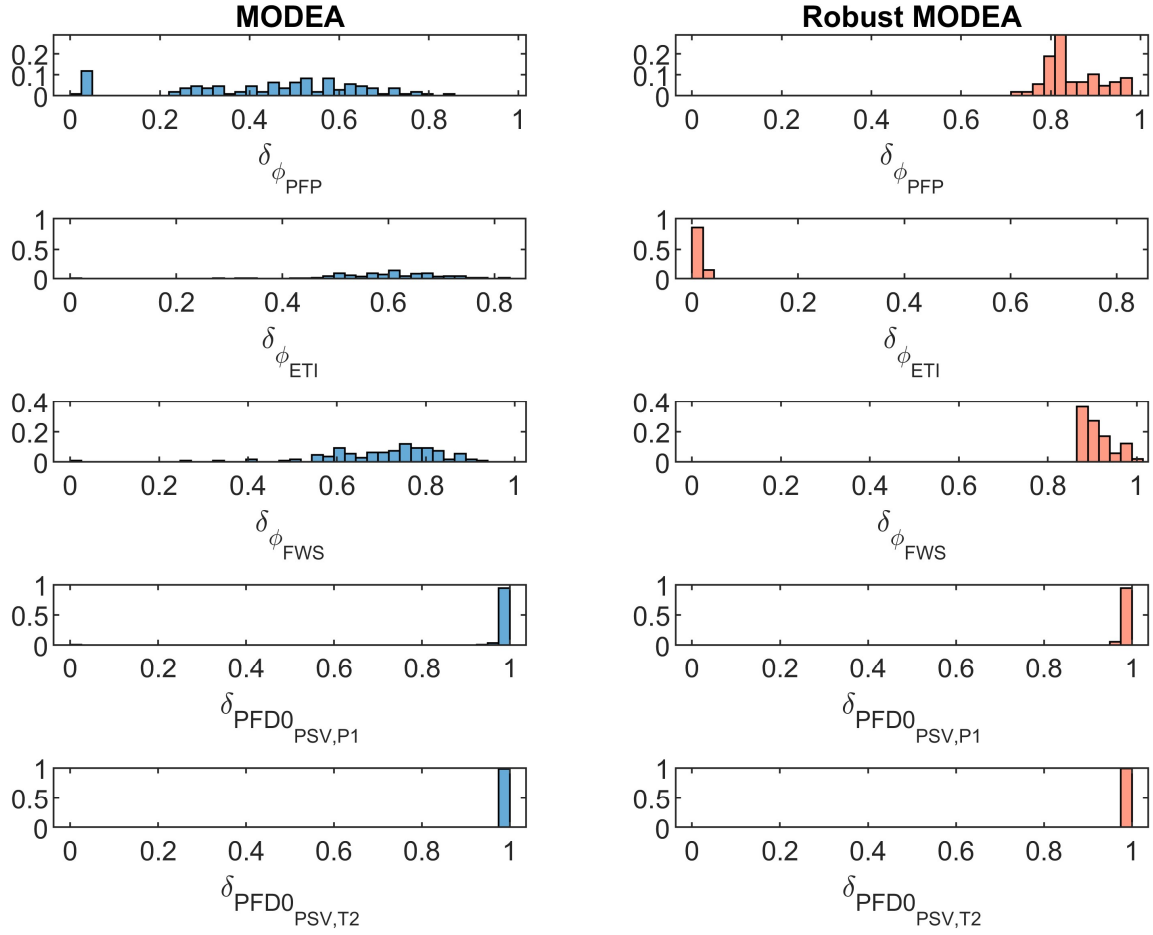

Fig. 7. Histograms of the PDF of δ_d from the robust (orange) and non-robust (blue) PF of MODEA.

From the results presented it is possible to conclude that:

- The performance parameters of PFP, FWS and PSV (of both tanks) are of utmost importance, and the decision maker should allocate resources for their improvement, whose amount can be estimated following the guidelines provided in Section 3.3.

- The uncertainty of the dynamic model parameters cannot be neglected, since, without the robustness constraint, ETI would result to deserve an improvement, whereas PFP would not. This discrepancy between the non-robust and the robust solutions (in which, instead, PFP is identified as one of the barriers to be improved the most, at the expense of ETI), is due to the necessary assumptions on the uncertainty in the response time, that is large for ETI and null for PFP, leading to a much larger uncertainty on Π if ETI is preferred over PFP. Therefore,

without considering the uncertainties, no resources would be allocated to improve PFP, leading to a larger uncertainty on the mitigative power and, therefore, to a larger risk of severe consequences in case of earthquake; whereas, improving the parameters following the expectations of the robust PF leads to solutions that are less affected by the uncertainties, allowing a proper management of the NaTech risk.

5. Conclusions

In this work, a novel MOO framework has been presented to identify the improvements on the safety barriers performance parameters necessary to obtain the largest mitigation of a NaTech scenario at the lowest cost. The accidental scenario evolution is assessed with a dynamic phenomenological model able to calculate a tailored performance metric, defined to represent the mitigative power of the system. Also, the uncertainty of the parameters of the dynamic model is accounted for with the introduction of a constraint for robust optimization. Different MOO algorithms are benchmarked to find the most suited to address the problem of identifying a robust PF, composed only by solutions that are only marginally affected by the uncertain parameters perturbation.

The proposed framework has been tested on a case study of literature regarding a chemical facility exposed to NaTech scenarios caused by earthquakes. The results obtained show the capability of the framework in identifying the safety barriers whose improvement is most relevant to optimally manage the risk arising from NaTech scenarios. Furthermore, when giving due account to the uncertainty in the dynamic model parameters, the improvement of the performance of the passive barrier becomes necessary to obtain robust optimal solutions, whereas this would have been overlooked if the decision would have been taken neglecting such uncertainty.

Appendix. MOO algorithms

Non-dominated Sorting Genetic Algorithm II

NSGA-II is a Multi-Objective Evolutionary Algorithm (MOEA) comprised of the following steps [8]:

1. Generate an initial random population $p^{g=1}$ (of size NP_N) of candidate solutions, which are vectors (also called chromosomes) whose components are the decision variables. The index g represents the generation number.

2. While the maximum number of generations is not reached:

    a. Generate an intermediate population $p^{g'}$ by applying the tournament selection operator to the parent population p^g.

    b. Generate an offspring population o^g by applying the evolution operators of crossover (with rate CR_N) and mutation (with rate MR) to the intermediate population $p^{g'}$.

    c. Combine the parent and offspring population to obtain a union population u^g.

    d. Evaluate the fitness of the chromosomes of u^g.

    e. Select the first NP chromosomes of u^g based on non-domination and crowding distance (with respect the values of the objective functions) to be the new parent population p^{g+1}.

Multi-Objective Differential Evolution Algorithm

MODEA is a state-of-practice MOEA, comprised of the following steps [9]:

1. Generate an initial random population (of size NP_M) of vectors $x_n^{g=1}$, each representing a candidate solution. The index g represents the generation number.

2. While the maximum number of generations is not reached:

    a. For each x_n^g belonging to the *g-th* generation, apply the mutation operator to generate a noisy vector v_n^{g+1} as follows:

    $$v_n^{g+1} = x_n^g + (x_{r,1}^g - x_{r,2}^g) \cdot F \tag{18}$$

    where $x_{r,1}$ and $x_{r,2}$ are vectors randomly chosen from the population and F is a scaling factor.

    b. For each pair $\left(x_n^g, v_n^{g+1}\right)$, apply the crossover operator (with rate CR_M) to generate the components a trial vector u_n^{g+1} as follows:

    $$u_{n,z}^{g+1} = \begin{cases} v_{n,z}^{g+1} & if \ rand(z) \le CR_M \ or \ z = rnbr(n) \\ x_{n,z}^g & if \ rand(z) > CR_M \ and \ z \ne rnbr(n) \end{cases} \tag{19}$$

where $rand(z)$ is the z-th evaluation of a uniform random number generator with outcome $\in [0,1]$ and $rnbr(n)$ is a randomly chosen index which ensures that at least one component of v_n^{g+1} is given to u_n^{g+1}.

   c. For each pair (x_n^g, u_n^{g+1}), select the fittest vector between the two to keep in the population.

Multi-Objective Particle Swarm Optimization

MOPSO is a swarm intelligence algorithm that takes inspiration from the behavior of bird flocks and is composed by the following steps [10]:

1. Generate an initial population (of size NP_P) of candidate solutions $POP_n^{g=1}$ (also called particles) with random positions (whose components are the decision variables) and velocity. The index g represents the iteration number.

2. While the maximum number of iterations is not reached:

   a. Evaluate the fitness of each of the particle and store in a repository REP^g (of size NR_P) the positions of the particles that represent non-dominated vectors in the objective space. If the repository is full, prioritize the solutions located in less populated areas of the objective space.

   b. For each particle, store its best position (in terms of fitness) across the generations as $PBEST_n^g$.

   c. Compute the velocity of each particle as follows:

$$VEL_n^{g+1} = W \cdot VEL_n^g + R_1 \cdot \left(PBEST_n^g - POP_n^g\right) + R_2 \cdot \left(REP_h^g - POP_n^g\right) \quad (20)$$

Where W is the inertia weight, R_1 and R_2 are random numbers uniformly generated in the range $[0,1]$ and REP_h^g is the position of a solution from the repository, whose index h is chosen with a roulette-wheel selection.

   d. Compute the new positions of the particles as follows:

$$POP_n^{g+1} = POP_n^g + VEL_n^{g+1} \quad (21)$$

   e. Amend the particles to remain in the boundaries of the decision variables.

Multi-objective Salp Swarm Algorithm

MSSA is a swarm intelligence algorithm that takes inspiration from the behavior of salp chains and is composed by the following steps [11]:

1. Generate an initial population (of size NP_S) of candidate solutions s_n^g (called salps) with random positions (whose components are the decision variables). The index g represents the iteration number.

2. While the maximum number of iterations is not reached:

a. Calculate the fitness of each salp and add to the repository (of size NR_s) the non-dominated salps. If the repository is full, prioritize the solutions located in less populated areas of the objective space.

b. Choose a source of food F^g from the repository.

c. Update the $z=1,2,...Z$ components of the position of the leading salp (the first of the chain) as follows:

$$s_{1,z}^{g+1} = \begin{cases} F_z^g + c_1\big((ub_z - lb_z)c_2 + lb_z\big) \; if \; c_3 \geq 0 \\ F_z^g - c_1\big((ub_z - lb_z)c_2 + lb_z\big) \; if \; c_3 < 0 \end{cases} \tag{22}$$

where $c_1 = 2e^{-\left(\frac{4g}{G}\right)^2}$ (with G being the maximum number of iterations), c_2 and c_3 are random numbers uniformly generated in the range $[0,1]$ and ub_z and lb_z are the upper bound and lower bound of the z-th decision variable, respectively.

d. Update the $z=1,2,...Z$ components of the positions of the rest of the salps as follows:

$$s_{n,z}^{g+1} = \frac{1}{2}\big(s_{n,z}^g - s_{n-1,z}^{g+1}\big) \tag{23}$$

e. Amend the salps to remain in the boundaries.

References

[1]   N. Khakzad and P. van Gelder, "Vulnerability of industrial plants to flood-induced natechs: A Bayesian network approach," *Reliability Engineering and System Safety*, vol. 169, pp. 403–411, Jan. 2018, doi: 10.1016/j.ress.2017.09.016.

[2]   N. Khakzad and V. Cozzani, "Special issue: Quantitative assessment and risk management of Natech accidents," *Reliability Engineering and System Safety*, vol. 203. Elsevier Ltd, Nov. 01, 2020. doi: 10.1016/j.ress.2020.107198.

[3]   A. Misuri, G. Landucci, and V. Cozzani, "Assessment of safety barrier performance in the mitigation of domino scenarios caused by Natech events," *Reliability Engineering and System Safety*, vol. 205, Jan. 2021, doi: 10.1016/j.ress.2020.107278.

[4]   A. Misuri, G. Landucci, and V. Cozzani, "Assessment of safety barrier performance in Natech scenarios," *Reliability Engineering and System Safety*, vol. 193, Jan. 2020, doi: 10.1016/j.ress.2019.106597.

[5]   A. Misuri and V. Cozzani, "A paradigm shift in the assessment of Natech scenarios in chemical and process facilities," *Process Safety and Environmental Protection*, vol. 152, pp. 338–351, Aug. 2021, doi: 10.1016/J.PSEP.2021.06.018.

[6]   M. Marseguerra, E. Zio, and S. Martorell, "Basics of genetic algorithms optimization for RAMS applications," *Reliability Engineering and System Safety*, vol. 91, no. 9, pp. 977–991, Sep. 2006, doi: 10.1016/j.ress.2005.11.046.

[7]   K. Deb and H. Gupta, "Introducing Robustness in Multi-Objective Optimization."

[8]   K. Deb, A. Pratap, S. Agarwal, and T. Meyarivan, "A fast and elitist multiobjective genetic algorithm: NSGA-II," *IEEE Transactions on Evolutionary Computation*, vol. 6, no. 2, pp. 182–197, Apr. 2002, doi: 10.1109/4235.996017.

[9]   R. Storn and K. Price, "Differential Evolution-A Simple and Efficient Heuristic for Global Optimization over Continuous Spaces," Kluwer Academic Publishers, 1997.

[10]   C. A. Coello Coello and M. S. Lechuga, "MOPSO: A proposal for multiple objective particle swarm optimization," in *Proceedings of the 2002 Congress on Evolutionary Computation, CEC 2002*, 2002, vol. 2, pp. 1051–1056. doi: 10.1109/CEC.2002.1004388.

[11]   S. Mirjalili, A. H. Gandomi, S. Z. Mirjalili, S. Saremi, H. Faris, and S. M. Mirjalili, "Salp Swarm Algorithm: A bio-inspired optimizer for engineering design problems," *Advances in Engineering Software*, vol. 114, pp. 163–191, Dec. 2017, doi: 10.1016/j.advengsoft.2017.07.002.

[12]   K. Deb and K. Deb, "Evolutionary Optimization in Multi-objective Optimal Control View project Tomographic Reconstruction by Evolutionary Optimization Techniques View project Multi-Objective Optimization Using Evolutionary Algorithms: An Introduction," 2001. [Online]. Available: http://www.iitk.ac.in/kangal/deb.htm

[13]   R. Sarker and C. A. Coello Coello, "Assessment Methodologies for Multiobjective Evolutionary Algorithms," in *Evolutionary Optimization*, Kluwer Academic Publishers, 2006, pp. 177–195. doi: 10.1007/0-306-48041-7_7.

[14] J. Wu and S. Azarm, "Metrics for quality assessment of a multiobjective design optimization solution set," *Journal of Mechanical Design, Transactions of the ASME*, vol. 123, no. 1, pp. 18–25, Mar. 2001, doi: 10.1115/1.1329875.

[15] Lizàrraga Lizàrraga Giovanni, Hernàndez Aguirre Arturo, and Botello Rionda Salvador, *G-Metric: an M-ary Quality Indicator for the Evaluation of Non-dominated Sets*.

[16] E. Zitzler, K. Deb, and L. Thiele, "Comparison of Multiobjective Evolutionary Algorithms: Empirical Results."

[17] L. Ding, F. Khan, and J. Ji, "A novel vulnerability model considering synergistic effect of fire and overpressure in chemical processing facilities," *Reliability Engineering and System Safety*, vol. 217, Jan. 2022, doi: 10.1016/j.ress.2021.108081.

[18] A. Zidan, S. Tappe, and T. Ortmaier, "A comparative study on the performance of MOPSO and MOCS as auto-tuning methods of PID controllers for robot manipulators," in *ICINCO 2018 - Proceedings of the 15th International Conference on Informatics in Control, Automation and Robotics*, 2018, vol. 1, pp. 240–247. doi: 10.5220/0006899802400247.

[19] Yong Qin, Limin Jia, Jianghua Feng, Min An, and Lijun Diao, *Proceedings of the 2015 International Conference on Electrical and Information Technologies for Rail Transportation*. 2015.

[20] G. Landucci, F. Argenti, A. Tugnoli, and V. Cozzani, "Quantitative assessment of safety barrier performance in the prevention of domino scenarios triggered by fire," *Reliability Engineering and System Safety*, vol. 143, pp. 30–43, Aug. 2015, doi: 10.1016/j.ress.2015.03.023.

[21] A. Misuri, G. Landucci, and V. Cozzani, "Assessment of risk modification due to safety barrier performance degradation in Natech events," *Reliability Engineering and System Safety*, vol. 212, Aug. 2021, doi: 10.1016/j.ress.2021.107634.

[22] S. Mukherjee, R. Nateghi, and M. Hastak, "A multi-hazard approach to assess severe weather-induced major power outage risks in the U.S.," *Reliability Engineering & System Safety*, vol. 175, pp. 283–305, Jul. 2018, doi: 10.1016/J.RESS.2018.03.015.

[23] C. Wade, M. Spearpoint, A. Bittern, and K. W. H. Tsai, "Assessing the sprinkler activation predictive capability of the BRANZFIRE fire model," *Fire Technology*, vol. 43, no. 3, pp. 175–193, Sep. 2007, doi: 10.1007/s10694-007-0009-5.

[24] Q. Li, "Estimation of fire detection time," in *Procedia Engineering*, 2011, vol. 11, pp. 233–241. doi: 10.1016/j.proeng.2011.04.652.

[25] V. G. Zverev, V. I. Zinchenko, and A. F. Tsimbalyuk, "Physical and mechanical properties and thermal protection efficiency of intumescent coatings," in *IOP Conference Series: Materials Science and Engineering*, Jun. 2016, vol. 124, no. 1. doi: 10.1088/1757-899X/124/1/012109.

[26] B. C. R. Ewan, "A Study of Pressure Safety Valve Response Times under Transient Overpressures."

[27] Ministero dell'Interno, "ANNUARIO STATISTICO DEL CORPO NAZIONALE DEI VIGILI DEL FUOCO," 2019. [Online]. Available: www.vigilifuoco.it

[28] F. Di Maio, S. Marchetti, and E. Zio, "A framework of sensitivity analysis for the performance assessment of safety barriers impacted by NaTech accidents," *Submitted to Process Safety and Environmental Protection*, 2022.

[29]   G. Wehmeier and K. Mitropetros, "Fire protection in the chemical industry," *Chemical Engineering Transactions*, vol. 48, pp. 259–264, 2016, doi: 10.3303/CET1648044.

[30]   J. O. Ejeh, S. Liu, and L. G. Papageorgiou, "Multi-objective optimisation for safe multi-floor process plant layout using the Dow's Fire & Explosion Index," *Journal of Loss Prevention in the Process Industries*, vol. 76, May 2022, doi: 10.1016/j.jlp.2021.104722.

[31]   H. X. Ju, Z. J. Yu, and X. D. Xing, "Influence of fireproof damage on structural performance of post-installed anchor joint subjected to post-earthquake fire," in *IOP Conference Series: Materials Science and Engineering*, Sep. 2019, vol. 592, no. 1. doi: 10.1088/1757-899X/592/1/012128.

[32]   N. Khakzad, G. Landucci, V. Cozzani, G. Reniers, and H. Pasman, "Cost-effective fire protection of chemical plants against domino effects," *Reliability Engineering and System Safety*, vol. 169, pp. 412–421, Jan. 2018, doi: 10.1016/j.ress.2017.09.007.

[33]   T. Okamoto and Y. Kuwata, "Influence to Water Outage due to Damage to Regional Water Supply during the 2011 off the Pacific Coast of Tohoku Earthquake," 2012.

[34]   Y. Hamadi, E. Monfroy, and F. Saubion, *Evolutionary algorithms parameters and methods to tune them*, vol. 9783642214349. Springer-Verlag Berlin Heidelberg, 2013. doi: 10.1007/978-3-642-21434-9.

[35]   M. Erik and H. Pedersen, "Good Parameters for Particle Swarm Optimization."